Separating Greenhouse-Gas Driven Forcing from Natural Fluctuations in the Time Series for Global Mean Temperatures

Cyrus C. Taylor*
Department of Physics, Case Western Reserve University, Cleveland, Ohio 44106, USA

(Received 9 April 2025; revised 2 October 2025; accepted 9 February 2026; published 12 March 2026)

The year 2024 was the hottest in the modern era, followed by 2023. Do these temperatures signal unexpected changes in the climate system? Writing the global annual mean temperature as the sum of two terms, greenhouse-gas driven climate change and fluctuations due to internal and external variability, we model the first term by extending the logarithmic dependance of the temperature anomaly to non-equilibrium conditions. We validate the method using the illustrative scenarios considered by the IPCC. Fitting the data, we find that the residuals for 2023 and 2024 are consistent with past fluctuations. We comment on how putative changes in the climate regime will manifest themselves in coming years.

DOI: 10.1103/897x-zrmv

Introduction—The annually averaged global mean surface temperature in 2024 was the highest in the modern instrumental era [1], and likely for much longer than that; 2023 was close behind. We expect temperatures to continue to rise inexorably as long as we continue to emit greenhouse gases into the atmosphere, but the past two years were sufficiently striking that it is necessary to ask, *do these temperatures signal unexpected changes in the climate system?*.

This question was addressed at a special session on "Cracking the Puzzle of the Anomalous Temperatures in 2023" at 2024 annual meeting of the American Physical Society [2,3]. The World Meteorological Organization also addressed the question in its report on the "State of the Climate 2024" [4]. In both cases, the emphasis was on estimating the magnitude of various factors such as the onset of El Niño, changes in the regulation of shipping aerosols, the rapid onset of Solar Cycle 25, and the Hunga Tonga volcanic explosion.

In this Letter we take a different approach. We first establish a simple framework for modeling the change in the global mean temperature due to changing concentrations of greenhouse gases in the atmosphere. We then examine the distribution of observed temperatures relative to this model. These residuals correspond to fluctuations due to internal and external variability of the climate system. This approach allows us to ask whether or not these fluctuations are consistent with those observed over the course of the past 65 years, since the advent of regular high quality CO_2 measurements at Mauna Loa.

Methodology—To address these questions we need to disentangle effects of climate change from the generic fluctuations in the climate system. We thus write the global mean temperature anomaly as the sum of two terms,

$$\Delta(t) = \theta(t) + w(t), \tag{1}$$

where $\Delta(t)$ is the global mean temperature relative to the average over a defined baseline period, $\theta(t)$ is the change in global mean temperature driven by the change in the atmospheric concentrations of greenhouse gases, and $w(t)$ captures the internal and external variability of the climate system, with $\langle w(t)\rangle = 0$. This approach is closely related to that of "fingerprinting" in attribution studies of the effects of climate change [5]. Here, however, rather than seeking to detect a signal in the presence of large background noise, we are rather seeking to isolate the fluctuations and to study their properties.

The challenge is that while we understand the physics of the climate system quite well, it is not yet possible to determine $\theta(t)$ from first principles with an accuracy small compared to the fluctuations represented by $w(t)$. Thus, for example, fluctuations are defined with respect to a Loess smoothing of the time series with a 20 year time constant in the analysis of [4]. Though well-grounded in techniques of data analysis, this approach does not incorporate the most important thing that we know about anthropogenic climate change: the baseline is driven by changes in greenhouse gas concentrations in the atmosphere.

We pursue an alternative approach, based on the fact that $\theta(t)$ is approximately logarithmic with respect to the atmospheric carbon dioxide concentration [6–10], a result known since Arrhenius [11]. As usually presented, this is a

*Contact author: cct@case.edu

statement about equilibrium temperatures. We extend it here to consider situations, such as those at the present time, where the Earth's radiation budget is out of balance. Further, as there is a strong correlation between the overall forcing of all greenhouse gases with that of CO_2 ($r = 0.996$ for NOAA's Annual Atmospheric Greenhouse Gas dataset [12] covering the years 1979–2024), we will use the atmospheric CO_2 concentration as a proxy for the combined effects of all greenhouse gases.

We validate the resulting model by showing that it can be used to fit the five main scenarios used by the IPCC with errors that are not only small compared to the year-to-year variability of the Earth's global mean temperature, but are also small compared to the uncertainties in the determination of the global mean temperature.

Our starting point is a simple energy balance model. If the absorbed solar radiation, A, exceeds the infrared radiation radiated to space, then the balance goes to warming the Earth. If Φ is the Earth's energy imbalance per square meter, i.e., the net radiative energy flux at the top of the atmosphere, and Q is the average total heat content of the Earth's climate system per square meter, then

$$\Phi = \frac{dQ}{dt} = c_E \frac{d\theta}{dt}, \tag{2}$$

where c_E is the effective heat capacity per square meter of the Earth's climate system (assumed to be constant on the timescales of interest to us here), and where we neglect fluctuations $w(t)$. The temperature anomaly is thus proportional to the cumulative integral of the energy imbalance. We can thus use the estimates for total change in the heat content of the Earth's climate system to estimate $c_E = 24.3 \pm 3.9$ watt years$/(m^2\ \mathrm{K})$ [13].

Introducing T_e as the effective emission temperature of the Earth, we then have

$$c_E \frac{d\theta}{dt} = A - \sigma T_e^4, \tag{3}$$

where σ is the Stefan-Boltzmann constant.

If we want to consider dynamics near equilibrium, we can introduce an equilibrium emission temperature $\bar{T}_e$ given by

$$\bar{T}_e = \left(\frac{A}{\sigma}\right)^{1/4}. \tag{4}$$

One can then ask how the emission temperature will change under changes in the Earth's mean surface temperature, θ, and under changes in the greenhouse gas concentration of the atmosphere.

Following Pierrehumbert [7] [p. 149], it is useful to introduce the notion of an effective radiating level of the atmosphere, corresponding to the characteristic depth from which infrared radiation escapes to space. For fixed greenhouse gas concentrations, the radiating level stays essentially fixed as temperature varies [7] [p. 265]. Hence, assuming a linear lapse rate for the atmosphere, a change in surface temperature implies a corresponding change in the emission temperature. Conversely, as more greenhouse gas is added to the atmosphere, more of the lower parts of the atmosphere become opaque to infrared radiation, increasing the altitude of the effective radiating level, and hence, for fixed atmospheric temperature profile, a reduction in the emission temperature. The resulting change in outgoing long wavelength radiation is approximately logarithmic in the CO_2 concentration [7] [p. 225]. The two effects of interest to us—the change in outgoing long wavelength radiation due to a change in surface temperature, and the change in outgoing long wavelength radiation due to a change in CO_2 concentration in the atmosphere—can thus be incorporated for small changes in θ or in the CO_2 concentration by taking

$$T_e = \bar{T}_e + \theta - \lambda \ln(c/c_r) \tag{5}$$

for some λ (related to the climate sensitivity of the system) and some reference CO_2 concentration c_r.

Noting that $\overline{T_e} \approx 255$ K [14] [p. 32], while θ and $\lambda \ln(c/c_r)$ are of the order of a few degrees K at the most in the foreseeable future, the ratio

$$\frac{\theta - \lambda \ln(c/c_r)}{\overline{T}_e} \tag{6}$$

is of the order of 10^{-2} or less.

Substituting (5) into Eq. (3) and expanding in (6), we have

$$T_E^4 \approx \bar{T}_E^4 \left(1 + 4\left(\frac{\theta - \lambda \ln(c/c_r)}{\bar{T}_E}\right)\right) \tag{7}$$

It is convenient to introduce a time constant τ defined by

$$\tau = \frac{c_E \bar{T}_e}{4\sigma \bar{T}_e^4}, \tag{8}$$

that is, the total heat content in the climate system divided by the rate at which energy is radiated to space. We can then write (3) as

$$\tau \frac{d\theta}{dt} = -\theta + \lambda \ln(c/c_r), \tag{9}$$

where, using the value of c_E from above, we have $\tau = 6.4 \pm 1.0$ yr.

We then determine λ and c_r by solving (3), typically numerically, and vary the parameters (including the initial value θ_0) so as to minimize the rms deviation from the data.

Validation of methodology—We start by considering the five illustrative emissions trajectories used by the IPCC in

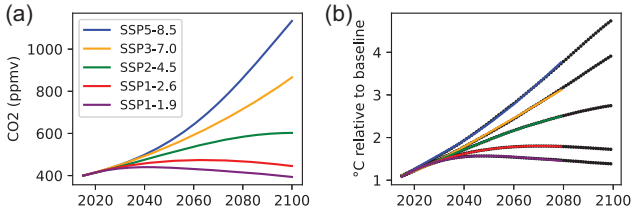

FIG. 1. (a) Projected CO_2 concentrations in the five illustrative emissions trajectories used by the IPCC in its sixth assessment report to explore the climate response to a broad range of greenhouse gas, land-use, and air pollutant futures [15,16]. (b) Corresponding global surface temperature. Solid lines indicate the values used by the IPCC based on CMIP6 model simulations [17]. The dotted lines are the fits of our model, based on Eq. (9), illustrating the ability of our simple model to accurately capture the results of more comprehensive simulations.

its sixth assessment report to explore the climate response to a broad range of greenhouse gas, land-use, and air pollutant futures [15,16], as illustrated in Fig. 1(a). Figure 1(b) illustrates the corresponding IPCC AR6 temperature trajectories [17] (solid lines) together with the results of the process of fitting solutions to Eq. (9) to this data using the reference CO_2 concentration pathways as input. As we only have annual CO_2 data from Mauna Loa for 1959-2024, we consider fits to the IPPC scenarios over a period of corresponding length (2015-2080).

The parameters for these fits are reported in Table I. Of these, the most interesting are the values of λ for each of the scenarios which differ among themselves, as well as from the value determined from data (see below in the analysis section). This is not surprising as each scenario has its own distinct changing mix of greenhouse gases and other characteristics. What is important for our present purposes is that our simple model is able to reproduce the results of each scenario using only CO_2 as a proxy for the overall mix.

The rms error across the five scenarios is 0.007 C. This is more than an order of magnitude smaller than the standard deviation of the residuals, and it is about half the size of the uncertainty of 0.013 C in the 2024 global mean temperature reported by the WMO [1]. We thus expect that this procedure can reproduce the actual temperature trajectories with sufficient precision to study the temperature fluctuations $w(t)$ through the residuals of the measured values of Δ with respect to the fit $\theta(t)$.

Data—We now turn to the real world. The longest record of direct measurements of atmospheric CO_2 concentrations are from the Mauna Loa Observatory [18]. It will be useful later that the data is well described by

$$c(t) = c_0 + c_1 e^{\alpha t}, \tag{10}$$

where, fitting to the entire Mauna Loa dataset, we find $c_0 = 255.46 \pm 0.36$ ppm, $c_1 = 59.26 \pm .33$ ppm, and $\alpha = 0.01611 \pm .00006$ per year. The data and the fit are illustrated in Fig. 2(a).

TABLE I. Parameters of the solutions to Eq. (9) for fits of the global mean surface temperatures to each of the five IPCC AR6 illustrative emissions trajectories [17] using the corresponding reference CO_2 concentrations [15,16] as inputs.

Scenario	λ	c_r	θ_0
SSP5-8.5	3.65	275.9	1.08
SSP3-7.0	3.69	287.4	1.11
SSP2-4.5	3.48	277.7	1.10
SSP1-2.6	3.03	260.7	1.09
SSP1-1.9	2.95	257.3	1.08

For the global mean temperature, we use the average of GISTEMP [19], NOAA [20], Berkeley Earth [21], HadCRUT5 [22], and ERA5 [23] data. The various groups report anomalies relative to varying baselines. The UK Met Office Climate Dashboard calculates anomalies relative to a 1981-2010 baseline for all of them and then offsets by 0.69 C as the best estimate for that period relative to the standard 1850-1900 reference period used by the IPCC in the Sixth Assessment Report. We thus use the data sets as reported by the UK Met Office [24].

Analysis—Figure 2(b) shows the resulting fit of the global mean temperature data to the Mauna Loa CO_2 data; $\lambda = 4.55 \pm 0.19$ C, $c_r = 303.9 \pm 2.4$ ppm, and $\theta_0 = \theta(t = 1959) = 0.27 \pm 0.06$ C. The equilibrium climate sensitivity, that is, the temperature increase corresponding to long-term doubling of the atmospheric CO_2 concentration, is thus $\lambda \ln(2) = 3.16 \pm 0.14$ C, in close accord with the IPCC AR6 conclusion that the "best estimate is 3 °C with a likely range of 2.5 °C to 4 °C (high confidence)" [25].

Figure 2(c) plots the residuals of the data relative to the fit, plotted as a function of time. Note that the years 2021-2024 are denoted by red dots.

Figure 2(d) is a histogram of the residuals. The most recent four years, 2021-2024, are again illustrated in red. While 2024 has the greatest residual, it is only marginally higher than that of the second greatest year. Indeed, the difference between the two largest residuals (2024 at 0.204 C, and 1981 at 0.196 C) is less than the uncertainty in measurement of the global mean temperature.

Possible changes in the distribution of fluctuations around $\theta(t)$—As we noted in the Introduction, many factors are known to be correlated with fluctuations about $\theta(t)$, but it is difficult to quantify them. Indeed, it is our hope that our approach will help provide a systematic framework for evaluating the relative importance of various factors. For now, though, we merely try to glean what we can from the distribution of residuals about the fit $\theta(t)$.

One can use tests such as the Kolmogorov-Smirnov two-sample test [26] to ask if the distribution of residuals in the first half of the time period is consistent with that in the second. One finds a Kolmogorov-Smirnov statistic of 0.21, corresponding to a p value of 0.45. This provides no reason

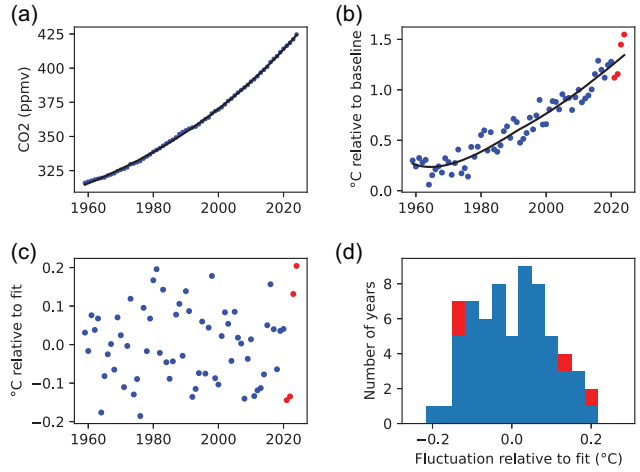

FIG. 2. (a) Annual mean CO_2 concentrations, as measured on Mauna Loa [18], together with fits to the data using the form of Eq. (10). Note that the fit to the data using only the years 1959-2000 does an excellent job of also parameterizing the data for the full period 1959-2024. (b) Annual global mean temperatures (average of GISTEMP, NOAA, Berkeley Earth, HadCRUT5, and ERA5), together with a fit to the data using the Mauna Loa CO_2 data as an input to Eq. (9). (c) Fluctuations in the annual mean temperature due to nonclimatic fluctuations. More specifically, the dots represent the difference between the annual global mean temperatures and the corresponding fit to CO_2 concentrations, as illustrated in (b). (d) Distribution of the residuals representing nonclimatic fluctuations. Blue indicates data from 1959 to 2020; red indicates data from 2021 to 2024.

to reject the hypothesis that the two distributions are the same.

This analysis implicitly assumes that the residuals are uncorrelated in time. We can check for autocorrelations at lag 1, for example, by using the Durbin-Watson test [27]. We find a Durbin-Watson statistic of $d = 1.570$, not inconsistent with our assumptions.

Of course, we hope that this Letter can be used in the future to better understand the nature of the fluctuations in terms of the dynamics of the climate system. It is thus interesting to examine the distribution of the changes of residuals. More precisely, Fig. 3(a) is a histogram of the distribution of $w_{i+1} - w_i$, where $w_i = \Delta_i - \theta(t_i)$. Figure 3(b) shows the correlations between successive changes.

While we do not at present have a model for what such fluctuations should look like, the rightmost panel of Fig. 3(a) looks anomalous compared to the rest. Interestingly, the bin includes two data points: the jump from 2022 to 2023 (0.27 C) and the jump from 1976 to 1977 (0.28 C). Figure 3(b) shows the correlations between successive changes in residuals. Whatever the underlying dynamics responsible for these changes, the fact that there are two comparable jumps almost 50 years apart suggests that the recent anomalous temperatures are not the result of some new process.

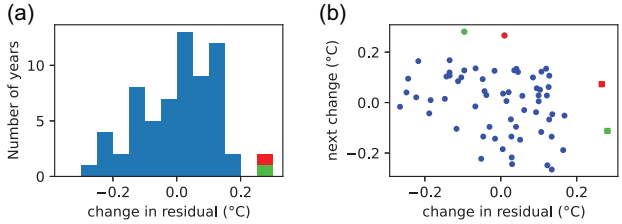

FIG. 3. (a) Distribution of the change in residuals from one year to the next. Green indicates the change from 1976 to 1977; red indicates the change from 2022 to 2023. (b) Correlations between successive changes in residuals.

Overall, the results appear to be consistent with the past pattern of fluctuations around the growing mean temperature driven by anthropogenic climate change.

Possible changes in the behavior of $\theta(t)$—One can illustrate how a change in the behavior of $\theta(t)$ would manifest itself by looking, not at the most recent data, but rather at data from the start of the Mauna Loa dataset. Indeed, while the Mauna Loa CO_2 data only begins in 1958, earlier data are available [28]. These show that there was an abrupt change in the character of CO_2 growth that began at about that time [see Fig. 4(a)], corresponding to the fact that it was at just this point that anthropogenic emissions from fossil fuels surpassed those from land use changes [29]. The growth in the atmospheric CO_2 concentration has been exponential since that time.

We note that Eq. (9) can be solved exactly for the CO_2 concentration given by (10):

$$\theta(t) = \lambda \ln\left(\frac{c}{c_r}\right) + \kappa e^{-\frac{t}{\tau}} + \alpha\tau\lambda\left({}_2F_1\left(1, \frac{1}{\alpha\tau}; 1 + \frac{1}{\alpha\tau}; -\frac{c_1 e^{\alpha t}}{c_0}\right) - 1\right). \quad (11)$$

Fitting this to the temperature anomaly data, we find $\lambda = 4.56 \pm 0.20$ C, $c_r = 304.0 \pm 2.4$ ppm, and $\kappa = 0.20 \pm 0.08$ C, in excellent agreement with the values we found earlier by direct numerical integration of Eq. (9) without making assumptions about the form of $c(t)$.

The term proportional to κ is a solution to the homogeneous equation $\tau d\theta/dt = -\theta$. That κ is nonzero reflects the fact that the temperature at the start of the Mauna Loa time series was higher than it would have been if the CO_2 concentration had been accurately described by Eq. (10) in the decades before the Mauna Loa measurements began, as illustrated in Fig. 4(a). It thus signals a change in the behavior of $\theta(t)$ due to the change in behavior of the rate of growth of the atmospheric CO_2 concentration.

If indeed we are now entering a new regime for warming, this past history suggests that we are in the very early stages of it. Any such change will become clear in coming years, over of a time period of the order of a few τ, and manifesting itself by a steady drift of the range of residuals upwards.

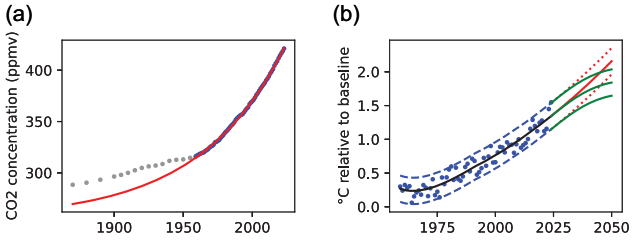

FIG. 4. (a) Mauna Loa CO_2 data [18] (blue dots), historical CO_2 data [28] (gray dots), and our model fit to the Mauna Loa data only (red line) showing the change in the rate of growth in atmospheric CO_2 that began in the late 1950s. (b) Temperature projections to 2050 in two scenarios, a continuing increase in the CO_2 concentration as given in (10) [red], and a scenario in which the current trajectory smoothly ameliorates to constant CO_2 concentrations after 2050 [green]. Dotted lines indicate the range of expected variation, $\pm 2\sigma$, where σ is the standard deviation of the residuals (dotted lines).

Of course we hope that there will be a change in regime, corresponding not to further accelerations in warming, but instead an arrest of it as the atmospheric greenhouse gases are stabilized. One can get an idea of how long it will take to be sure we are accomplishing these goals, as reflected in the global mean temperature, by considering Fig. 4(b), which shows the projected mean temperatures and range of variation over the course of the next quarter century in two scenarios: a continuing increase in the CO_2 concentration as given in (10), and a scenario in which the current trajectory smoothly ameliorates to constant CO_2 concentrations after 2050.

Closing remarks—Figure 4(b) illustrates two key points: first, that any changes in behavior of the climate system will take some years to clearly distinguish from the background fluctuations, and second, that this is not grounds for complacency. If we do not stop emitting greenhouse gasses, temperatures will continue inexorably to rise, further exacerbated from time to time by natural fluctuations.

Acknowledgments—This work was supported by the Albert A. Michelson Professor in Physics Endowment at Case Western Reserve University. The author thanks Dr. Evalyn Gates for many helpful conversations as the study progressed.

Data availability—The data that support the findings of this article are openly available [12,16–18,24,28, 29].

[1] WMO confirms 2024 as warmest year on record at about 1.55 °C above pre-industrial level (2025), https://wmo.int/news/media-centre/wmo-confirms-2024-warmest-year-record-about-155degc-above-pre-industrial-level.

[2] G. A. Schmidt, Z. Hausfather, D. Visioni, and M. Clyne, Cracking the puzzle of the anomalous temperatures in 2023: Observational and modeling studies to identify and understand potential factors and future implications I poster, in AGU24, Session GC23K (AGU, Washington, D.C., 2024), https://agu.confex.com/agu/agu24/meetingapp.cgi/Session/225040.

[3] G. A. Schmidt, Z. Hausfather, D. Visioni, and M. Clyne, Cracking the puzzle of the anomalous temperatures in 2023: Observational and modeling studies to identify and understand potential factors and future implications II oral, in AGU24, Session GC21O (AGU, Washington, D.C., 2024), https://agu.confex.com/agu/agu24/meetingapp.cgi/Session/233589.

[4] G. A. Schmidt and Z. Hausfather, Global mean surface temperature anomalies in 2023/2024, in *State of the Global Climate 2024*, WMO-No. 1368 (World Meteorological Association (WMO), Geneva, Switzerland, 2025), https://wmo.int/sites/default/files/2025-03/WMO-1368-2024_en.pdf.

[5] G. Hegerl and F. Zwiers, Use of models in detection and attribution of climate change, WIREs Climate Change **2**, 570 (2011).

[6] W. S. Broecker, Climatic change: Are we on the brink of a pronounced global warming?, Science **189**, 460 (1975).

[7] R. T. Pierrehumbert, *Principles of Planetary Climate* (Cambridge University Press, Cambridge, England, 2010).

[8] W. Zhong and J. D. Haigh, The greenhouse effect and carbon dioxide, Weather **68**, 100 (2013).

[9] M. Etminan, G. Myhre, E. J. Highwood, and K. P. Shine, Radiative forcing of carbon dioxide, methane, and nitrous oxide: A significant revision of the methane radiative forcing, Geophys. Res. Lett. **43**, 12614 (2016).

[10] D. M. Romps, J. T. Seeley, and J. P. Edman, Why the forcing from carbon dioxide scales as the logarithm of its concentration, J. Clim. **35**, 4027 (2022).

[11] S. Arrhenius, On the influence of carbonic acid in the air upon the temperature of the ground, London, Edinburgh, Dublin Philos. Mag. J. Sci. **41**, 237 (1896).

[12] NOAA Global Monitoring Laboratory, The noaa annual greenhouse gas index (aggi), https://gml.noaa.gov/aggi/aggi.html (2025) (accessed: 2026-01-09).

[13] K. von Schuckmann *et al.*, Heat stored in the earth system 1960–2020: Where does the energy go?, Earth Syst. Sci. Data **15**, 1675 (2023).

[14] D. Hartmann, *Global Physical Climatology*, International Geophysics (Elsevier Science, New York, 2015).

[15] IPCC, Summary for Policymakers, in *Climate Change 2021: The Physical Science Basis. Contribution of Working Group I to the Sixth Assessment Report of the Intergovernmental Panel on Climate Change*, edited by V. Masson-Delmotte, P. Zhai, A. Pirani, S. Connors, C. Péan, S. Berger, N. Caud, Y. Chen, L. Goldfarb, M. Gomis, M. Huang, K. Leitzell, E. Lonnoy, J. Matthews, T. Maycock, T. Waterfield, O. Yelekçi, R. Yu, and B. Zhou (Cambridge University Press, Cambridge, United Kingdom and New York, NY, USA, 2021), 10.1017/9781009157896.001.

[16] C. D. Jones, C. Koven, Z. Nicholls, S. Liddicoat, M. Meinshausen, and J. Lewis, Technical Summary of the Working Group I contribution to the IPCC sixth assessment report—input data for box TS.5, figure 1 (v20220817) (2023) NERC EDS Centre for Environmental Data Analysis, 10.5285/d6a301f3429b44e7924296f840f68fe6.

[17] C. D. Jones, C. Koven, Z. Nicholls, S. Liddicoat, M. Meinshausen, and J. Lewis, Summary for Policymakers

of the Working Group i Contribution to the IPCC Sixth Assessment Report—data for figure SPM.8 (v20210809) (2023) NERC EDS Centre for Environmental Data Analysis, 10.5285/98af2184e13e4b91893ab72f301790db.

[18] Data retrieved from https://gml.noaa.gov/ccgg/trends/data.html. Data Source: Dr. Xin Lan, NOAA/GML (http://gml.noaa.gov/ccgg/trends/) and Dr. Ralph Keeling, Scripps Institution of Oceanography (http://scrippsco2.ucsd.edu/).

[19] N. J. L. Lenssen, G. A. Schmidt, J. E. Hansen, M. J. Menne, A. Persin, R. Ruedy, and D. Zyss, Improvements in the GISTEMP uncertainty model, J. Geophys. Res. **124**, 6307 (2019).

[20] B. Huang, X. Yin, M. J. Menne, R. Vose, and H.-M. Zhang, Improvements to the land surface air temperature reconstruction in NOAAGlobalTemp: An artificial neural network approach, Artif. Intell. Earth Syst. **1**, e220032 (2022).

[21] R. A. Rohde and Z. Hausfather, The berkeley earth land/ocean temperature record, Earth Syst. Sci. Data **12**, 3469 (2020).

[22] C. P. Morice, J. J. Kennedy, N. A. Rayner, J. P. Winn, E. Hogan, R. E. Killick, R. J. H. Dunn, T. J. Osborn, P. D. Jones, and I. R. Simpson, An updated assessment of near-surface temperature change from 1850: The HadCRUT5 data set, J. Geophys. Res. **126**, e2019JD032361 (2021).

[23] H. Hersbach *et al.*, The ERA5 global reanalysis, Q. J. R. Meteorol. Soc. **146**, 1999 (2020).

[24] UK Met Office Climate dashboard: Get the data, https://climate.metoffice.cloud/temperature.html takes you to the climate dashboard data compilation.

[25] IPCC, Summary for policymakers, in *Climate Change 2021: The Physical Science Basis. Contribution of Working Group I to the Sixth Assessment Report of the Intergovernmental Panel on Climate Change*, edited by V. Masson-Delmotte, P. Zhai, A. Pirani, S. Connors, C. Péan, S. Berger, N. Caud, Y. Chen, L. Goldfarb, M. Gomis, M. Huang, K. Leitzell, E. Lonnoy, J. Matthews, T. Maycock, T. Waterfield, O. Yelekçi, R. Yu, and B. Zhou (Cambridge University Press, Cambridge, United Kingdom and New York, NY, USA, 2021), pp. 3–32, 10.1017/9781009157896.001.

[26] R. von Mises, Chapter ix—analysis of statistical data, in *Mathematical Theory of Probability and Statistics*, edited by R. von Mises (Academic Press, New York, 1964), pp. 431–493.

[27] J. Durbin and G. Watson, Testing for serial correlation in least squares regression. III, Biometrika **58**, 1 (1971).

[28] C. Smith, B. Hall, F. Dentener, J. Ahn, W. Collins, C. Jones, M. Meinshausen, E. Dlugokencky, R. Keeling, P. Krummel, J. Mühle, Z. Nicholls, and I. Simpson, IPCC Working Group 1 (WG1) Sixth Assessment Report (AR6) Annex III Extended Data, 10.5281/zenodo.5705391 (2021).

[29] P. Friedlingstein *et al.*, Global carbon budget 2024, Earth Syst. Sci. Data **17**, 965 (2025).